Journal of the Korean Society of Surveying, Geodesy, Photogrammetry and Cartography
Vol. 36, No. 1, 9-15, 2018
https://doi.org/10.7848/ksgpc.2018.36.1.9

ISSN 1598-4850(Print)
ISSN 2288-260X(Online)
Original article

Determination of Precise Regional Geoid Heights on and around Mount Jiri, South Korea

Lee, Suk-Bae[1)]

Abstract

Precise regional geoid heights on and around Mount Jiri were calculated and were compared to the KNGeoid14 (Korean National Geoid 2014) model. In this study, gravimetric geoid heights were calculated by using RCR (Remove-Compute-Restore) technique and then hybrid geoid heights were calculated by using the LSC (Least Square Collocation) method in the same area. In addition, gravity observation and GNSS(Global Navigation Satellite System) surveying performed in this study were utilized to determine gravimetric geoid heights and to compute hybrid geoid heights, respectively. The results of the study show that the post-fit error (mean and standard deviation) of hybrid geoid heights was evaluated as 0.057 ± 0.020 m, while the mean and standard deviation of the differences were -0.078 and 0.085 m, respectively for KNGeoid14. Therefore, hybrid geoid heights in this study show more considerable progress than KNGeoid14.

Keywords: GECO, Precise Regional Geoid Heights, RCR Technique, Hybrid Geoid Heights, GNSS/Leveling, Geoid Heights, Gravity Observation

1. Introduction

EGM2008 (Earth Geopotential Model 2008) is a global gravity field model developed by the NGA (National Geospatial-Intelligence Agency) in the USA that was made to be capable of analysing ultra-high degrees of spherical harmonics up to 2190 degrees (Pavlis *et al*., 2008). GECO (Goce and Egm2008 COmbination) is a global gravity model computed by incorporating the GOCE-only TIM R5 solution into EGM2008 (Gilardoni *et al*., 2016), and it is the latest earth geopotential model and made available by the ICGEM (International Center for Global Earth Models). GECO was developed based on the integration of the EGM2008 and of the GOCE (Gravity field and steady-state Ocean Circulation Explorer) satellite tracking data to be capable of analyzing ultra-high degrees of spherical harmonics up to 2190 degrees. The GECO model is estimated to be slightly more accurate than the EGM2008 model in comparison to the GNSS/leveling derived geoid heights (ICGEM GNSS/levelling, 2018). There have been several studies on the development of geoid model based on the low-frequency part of the geoid obtained from the EGM.2008 (Baek *et al*., 2014; Lee and Kwon, 2015; Lee and Lee, 2010; Lee *et al*., 2012). KNGeoid13 (Baek *et al*., 2014) and KNGeoid14 (Lee and Kwon, 2015) are also Korean official geoid model developed by NGII (National Geographic Information Institute) using EGM2008 model, and it is estimated that they are more accurate in the flat area than mountainous area. Therefore, in this study, spherical harmonic analysis was performed for EGM2008 and GECO under the same conditions and the results were compared to access the usefulness of the GECO model.

Received 2018. 01. 31, Revised 2018. 02. 09, Accepted 2018. 02. 28.
1) Member, Dept. of Civil Engineering, Gyeongnam National University of Science and Technology (E-mail: sblee@gntech.ac.kr)

If there is more gravity data in a region, more precise geoid can be calculated. Since KNGeoid14 is estimated to be less accurate in mountainous areas than in flat areas, the addition of gravity measurement data or GNSS/leveling data in mountainous areas will increase the accuracy of the geoid model. So, gravity observations and GNSS surveying were carried out to calculate precise regional geoid heights in the study area. In this study, Mount Jiri in the area of 35.0°N to 35.6°N by 127.4°E to 128.2°E was selected as the study area. Mount Jiri is located in Gyeongsangnam-do, Jeollabuk-do and Jeollanam-do in South Korea and is one of the three famous mountains. The final geoid heights calculated in this study were compared to the geoid heights of the KNGeoid14 to evaluate the performance.

The purpose of this study is to calculate precise regional geoid heights on and around Mount Jiri, and this study was carried out in accordance with the flow chart in Fig. 1. In the first step, gravimetric geoid heights based on GECO were calculated by using RCR technique, and in the second step, hybrid geoid heights were calculated by using LSC method on and around Mount Jiri.

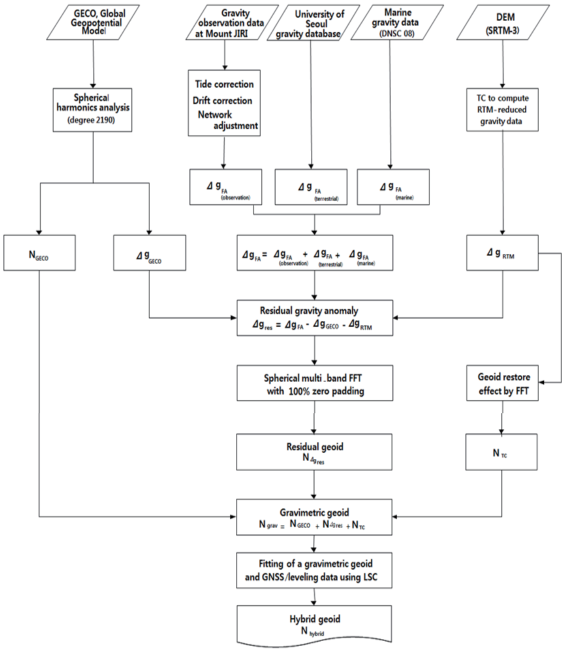

Fig. 1. Flow chart showing research methodology

2. Data and Methodology

The concept of the RCR technique implies that both topography and low-degree gravity signals are removed before computation and restored after Stokes' integration (Sjöberg, 2005). The geoid is estimated using Stokes' formulae with gravity anomaly, Δg, as input data. Before applying Stokes' formula, the gravity anomaly must be reduced by remove step of the RCR technique, Eq. (1)(Omang *et al*., 2000):

$$\Delta g_{res} = \Delta g_{FA} - \Delta g_{GGM} - \Delta g_{RTM} \tag{1}$$

where Δg_{FA} is the free-air anomaly, given as a point value at the surface of topography. Δg_{GGM} is the reference gravity anomaly and Δg_{RTM} is the terrain effect. The terrain effect, consisting of the Bouger plate, terrain correction and the indirect effect, is the volume integral of a disturbing mass anomaly (Forsberg, 1985). The gravimetric geoid is obtained after applying the restore step and geoid height can be computed by the following equation (Erol *et al*., 2009):

$$N_{grav} = N_{GGM} + N_{\Delta gres} + N_{RTM} \tag{2}$$

where N_{GGM} is the low-frequency part of the geoid obtained from the GGM (Global Geopotential Model). The medium-frequency part $N_{\Delta gres}$ of the geoid is the residual geoid computed from residual gravity anomalies using Stokes' integration. The residual gravity anomaly Δg_{res} remains in the gravity data after subtracting out the contributions of residual-terrain (Δg_{RTM}) and global-field (Δg_{GGM}) effects and the residual gravity anomaly is transformed into the residual geoid. The high-frequency part N_{RTM} of the geoid is the terrain effect on the geoid generated by the gravimetric reduction method using a DEM (Digital Elevation Model).

The reference gravity anomaly Δg_{GGM} and low-frequency geoid N_{GGM} were calculated by spherical harmonic analysis using both GECO and EGM2008 models up to degree and order 2190 under the same condition. For more accurate calculation of the free-air anomaly Δg_{FA}, 41 gravity observation data on and around Mount Jiri was added to the University of Seoul's gravity database (Baek *et al*., 2014; Hong *et al*., 2009). The terrain effect was calculated using the RTM

(Residual Terrain Model) method, which was more suitable for calculating topographic effect in the geoid determination of Korea (Lee and Lee, 2010), using a mean DEM surface with approximately 1′ × 1′ grid spacing and a Korean local DEM regenerated from SRTM (Shuttle Radar Topography Mission) data (SRTM, 2000). Thus, the gravimetric geoid heights over Mount Jiri were computed using the RCR technique with the application of a two-dimensional 4-band spherical FFT (Fast Fourier Transformation) (Forsberg and Sideris, 1993) on reduced-gravity data followed by the restoration of terrain effects and the GECO-model effect. Data was gridded in the area of 35.0°N to 35.6°N by 127.4°E to 128.2°E, at a basic grid spacing of 1′ × 1′ in latitude and longitude. The FFT was performed using 100% zero padding to limit periodicity effects and the computation of the geoid was done with the GRAVSOFT software developed by Forsberg and Tscherning (2008). The gravimetric geoid heights N_{GRAV} were calculated using Eq. (2) and the final hybrid geoid heights N_{Hybrid} which is corrected to gravimetric geoid heights with the correction term by fitting the 39 GNSS/leveling data were calculated. The correction term is modelled using the differences between GNSS/leveling derived geoid heights and gravimetric geoid heights. In this way a new geoid grid tuned to the levelling and GNSS datum can be obtained. The method of LSC is used for estimating the trend and modelling the residuals. For trend estimation, the 4-parameter model (Heiskanen and Moritz, 1967) was used. In the collocation process, a covariance function must be assumed for the residual geoid errors as a function of spherical distance. The 2nd order Markov covariance function (Iliffe *et al*., 2003) was used for determination of hybrid, Eq. (3), geoid in Mount Jiri:

$$C(s) = C_0 (1+\alpha s) e^{-\alpha s} \quad (3)$$

Such a covariance function is characterized by the zero variance C_0 and correlation length s, which determines the fit and the smoothness of the interpolated geoid error. The constant α is the only quantity to be specified, with C_0 automatically adapted to the data. In the selection of the correlation length and noise of observed errors, the user has a wide range of selection options. Either a strong fit to the GNSS data, or a more relaxed fit, which diminishes the impact of possible errors in the GNSS data (Tscherning *et al*., 2003). The correlation length was determined of 40 km approximately to each gravimetric geoids and 1 cm a priori GNSS noise was assumed.

3. Field Survey

3.1 Gravity observation

To obtain the geographic distribution of gravity, the measured gravity value should be corrected to the reference surface value through gravity reductions. Geoid is used as reference planes. Gravity observation was accomplished to determine precise regional geoid heights and GNSS surveying was also carried out not only to obtain a hybrid geoid, but also to evaluate the accuracy of the calculated geoid heights on and around Mount Jiri. Gravity observation was accomplished at 41 benchmarks on and around Mount Jiri using a CG5 digital gravimeter for the period of Feb. 23 to Mar. 07, 2015. The absolute gravity value at the observation stations was determined through tide correction and drift correction and in this process, the gravity values of Kwangjoo GA1, Geochang GA1 and Yeosoo GA1 were used as absolute reference stations. The standard error of the gravity value determined was 0.048 mGal, and this error was distributed to each station through least squares adjustment. The distribution of absolute gravity values in the study area was from 979528.490 mGal to 979763.133 mGal and the distribution of gravity anomaly calculated from the difference of normal gravity showed a distribution of 9.403 mGal at -231.297 mGal. The free-air anomaly at 41 benchmarks was calculated and combined with the University of Seoul's gravity database. The University of Seoul's gravity database contains 7,782 land gravity data and 534 gravity data acquired by PNU (Pusan National University) and JNU (Jinju National University) in 2009 and the accuracy of the gravity data is 0.488 mGal after cross-over adjustment (Lee and Kim, 2011). The network diagram of gravity measurements and absolute reference stations are shown in Fig. 2. Fig. 5 shows the detail of the Benchmark line at which gravity measurements were made. Fig. 3 shows the distribution of gravity anomalies calculated as a contour map

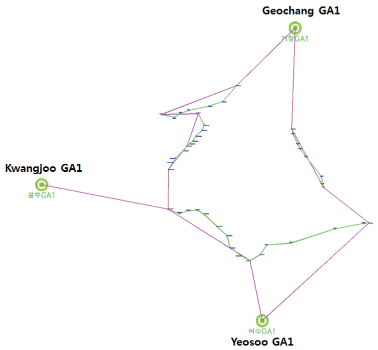

Fig. 2. Network diagram of gravity observation and adjustment

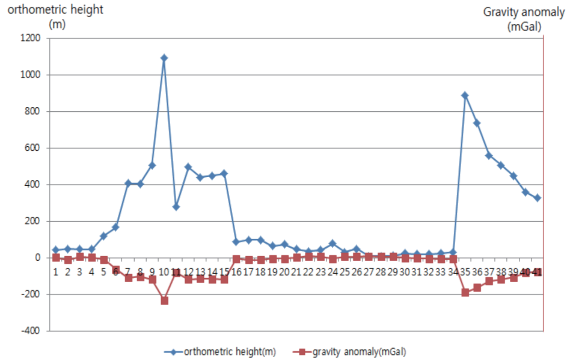

Fig. 4. The relation between orthometric heights and gravity anomalies

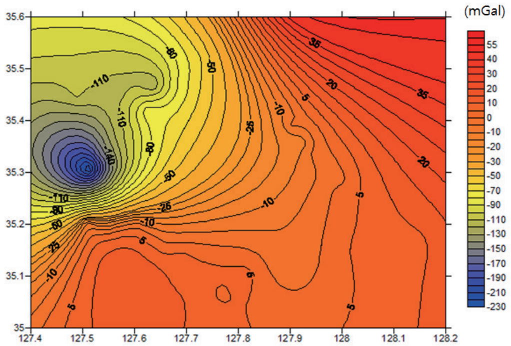

Fig. 3. Contour map of gravity anomaly calculated from gravity observations on and around Mount Jiri

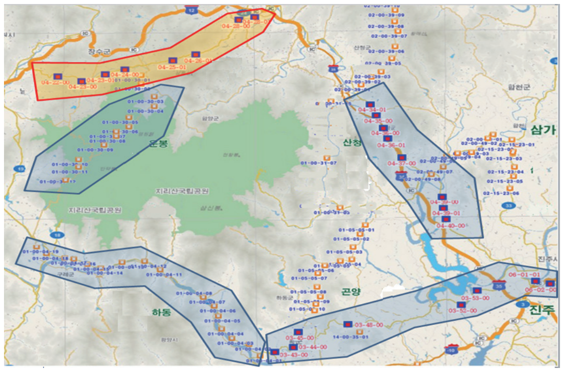

Fig. 5. Location map of GNSS surveying stations along the benchmark line

on and around Mount Jiri and the data was gridded in the area of 35.0°N to 35.6°N by 127.4°E to 128.2°E, at a basic grid spacing of 0.5′ × 0.5′ in latitude and longitude by Kriging method. Fig. 4 shows the relation between orthometric heights and gravity anomalies at 41 benchmark. In Fig. 4, the gravity anomaly value is the minimum value at the 10th point where the orthometric height is 1090 m which is the highest value and the gravity anomaly value is the maximum value at the 28th point where the orthometric height is the smallest. This figure shows an inverse relationship between orthometric heights and gravity anomalies.

3.2 GNSS surveying

GNSS surveying was carried out at 40 benchmarks as shown in Fig. 5 from Feb. 23 to 27, 2015. Three types of GNSS receivers which are Trimble R7, R8 and 5700 were used, and the GNSS occupation time was 2 hours. TBC (Trimble Business Center) ver.2.8 software was used for the baseline analysis and network adjustment of the GNSS data to determine ellipsoidal height. Finally, the ellipsoidal height of 39 benchmarks obtained after a quality test and GNSS/leveling derived geoid (N) was calculated using the official Benchmark height issued by the National Geographical by NGII using Eq. (4).

$$N = h - H \tag{4}$$

where h is the ellipsoidal height computed from GNSS data and H is the orthometric height. Lee *et al.* (2017) explained this process in detail, and the GNSS/leveling derived geoid showed a distribution of 26.667 to 28.330 m, and the mean and standard deviation were 27.679 m and 0.380 m, respectively.

Table 1. Statistics of four types of geoid heights calculated in this study (unit: m)

Division	Min.	Max.	Mean
EGM08 geoid (N_{EGM08})	25.567	27.848	27.065
GECO geoid heights (N_{GECO})	25.569	27.851	27.053
Gravimetric geoid heights (N_{GRAV})	25.538	28.027	27.203
Hybrid geoid heights (N_{Hybrid})	26.477	26.683	27.838

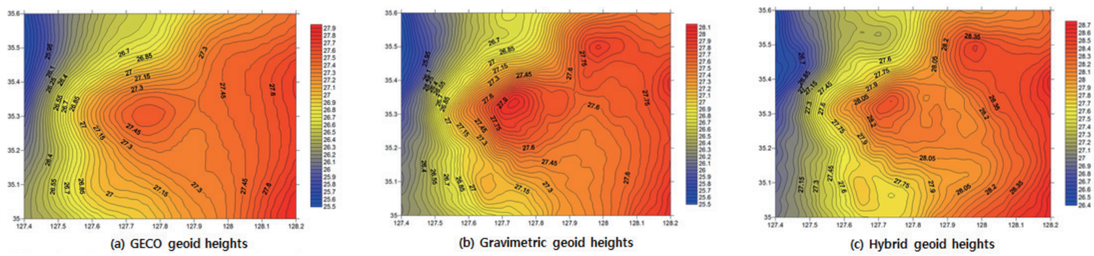

Fig. 6. Contour map of three types of geoid heights (unit: m)

4. Results and Evaluation

4.1 Results

In this study, four types of geoid heights were calculated. The first and second ones are the geoid heights calculated by spherical harmonic analysis using both EGM08 and GECO GGMs under the same condition, respectively. The third one is the gravimetric geoid heights calculated by the RCR technique. The fourth is a hybrid geoid height, made by combining gravimetric geoid height and GNSS/leveling derived geoid heights using the LSC method. Table 1 shows statistics for these four types of geoid heights, and the distribution of three types of geoid heights except EGM08 because the EGM08 geoid has already been introduced several times (Lee *et al*., 2012; Lee *et al*., 2017; Lee and Lee, 2010) are shown in Fig. 6 as a colored fill-in contour map. Fig. 6 (a) shows the distribution of low-frequency geoids (N_{GECO}) of the GECO Earth geopotential model, Fig. 6 (b) shows the results of gravimetric geoid heights (N_{GRAV}), as a contour map, and Fig. 6 (c) shows the contour distribution of hybrid geoid heights (N_{Hybrid}). Comparing the three figures in Fig. 6 clearly shows the contour change, which indicates that the calculations are well done.

4.2 Evaluation

For the evaluation, five types of geoid heights, which are the low-frequency part of the geoids (N_{EGM08} and N_{GECO}) obtained from EGM08 and GECO GGMs, respectively, the gravimetric geoid heights (N_{GRAV}), the hybrid geoid heights (N_{Hybrid}) and KNGeoid14 geoid heights are compared to GNSS/leveling derived geoid heights derived from the 39 GNSS/leveling data. The evaluation results are shown in Table 2 with statistics on the differences between the five types of geoid heights and GNSS/leveling derived geoid heights. Table 2 shows that GECO is slightly more accurate than EGM08 because the mean and standard deviation of the GECO geoid difference in the study area is smaller than those of EGM08. Therefore, if gravimetric geoid heights and hybrid geoid heights are calculated based on the low-frequency part of the geoids obtained from GECO, the accuracy of geoid heights is expected to be better.

As we can see in Table 2, the GECO geoid is the results of

Table 2. Statistics on the differences between the five types of geoid heights and GNSS/leveling derived geoid heights (m)

Division	Min.	Max.	Mean	Standard Deviation
EGM08 geoid (N_{EGM08}) – GNSS/leveling derived geoid	0.385	0.845	0.672	0.087
GECO geoid (N_{GECO}) – GNSS/leveling derived geoid	0.442	0.832	0.667	0.085
Gravimetric geoid (N_{GRAV}) – GNSS/leveling derived geoid	0.205	0.762	0.566	0.091
Hybrid geoid (N_{Hybrid}) – GNSS/leveling derived geoid	-0.223	0.094	0.057	0.020
KNGeoid14 – GNSS/leveling derived geoid	-0.406	0.105	-0.078	0.085

spherical harmonic analysis based on the GRS80 ellipsoid, and the mean of the differences between GECO geoid and GNSS/leveling derived geoid heights is 0.667 m, which is relatively large. The mean of the differences between gravimetric geoid heights and GNSS/leveling derived geoid heights is 0.566 m, which is also relatively large. It is judged that there is a bias between GECO GGM and GNSS/leveling derived geoid heights. However, the post-fit error (mean and standard deviation) of hybrid geoid heights was evaluated as 0.057 ± 0.020 m, while the mean and standard deviation of KNGeoid14 differences were -0.078 ± 0.085 m respectively, in the same area. These results show that the accuracy of the final hybrid geoid in the study area is greatly improved in comparison with KNGeoid14. Fig. 7 shows the differences between four types of geoid heights except EGM08 geoid and GNSS/leveling derived geoid heights as a line graph.

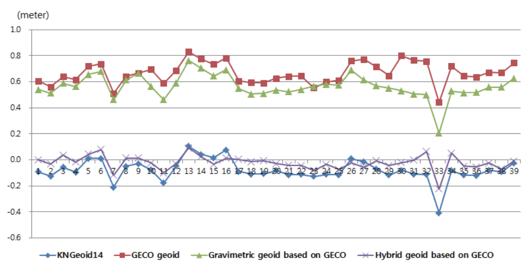

Fig. 7 Differences between the four types of geoid heights and GNSS/leveling derived geoid heights

5. Conclusion

In this study, spherical harmonic analysis was performed for GECO on and around Mount Jiri, for the first time, to access the usefulness of the GECO model. The results were compared to the results of the EGM08 model. By comparing GECO geoid with EGM08 geoid on and around Mount Jiri, it was found that GECO GGM is slightly more accurate than EGM08 GGM. This also suggests that if the geoid modeling is performed based on the GECO GGM, it can be more accurate than when based on the EGM08 GGM.

The purpose of this study was to calculate precise regional geoid heights on and around Mount Jiri. For the study, gravity observation was accomplished and these data were used in the calculation of gravimetric geoid heights. GNSS surveying was carried out at benchmarks then GNSS/leveling derived geoid heights were calculated, and also, these data were used for determination of hybrid geoid heights. The computation results show that the accuracy of the final hybrid geoid heights in the study area is greatly improved compared to KNGeoid14. This suggests that the addition of new gravity data and collocation of GNSS/leveling derived geoid heights in mountainous areas are very efficient in increasing the accuracy of geoid heights. However, since this study was conducted on a small area of Mount Jiri, it is necessary to conduct research on the whole of Korea in the future.

Acknowledgment

This work was supported by Gyeongnam National University of Science and Technology Grant in 2016.

References

Baek, K., Lee, J., Shin, G., Kwon, J.H., and Moon, J. (2014), Construction and precision verification of Korean national geoid model KNGeoid13, *Proceedings of the 2014 Spring Conference of the Korean Society of Surveying, Geodesy, Photogrammetry, and Cartography*, The Korean Society of Surveying, Geodesy, Photogrammetry, and Cartography, 24-25 April, Seoul, Korea, pp.111-114.

Erol, B., Sideris, M.G., and Çelik, R.N. (2009), Comparison of global geopotential models from the CHAMP and GRACE missions for regional geoid modeling in Turkey, *Study Geophysical Geodesy*, Vol. 53, pp. 419-441.

Forsberg, R. (1985), Gravity field terrain effect computation by FFT, *Bulletin Geodesy*, Vol. 59, pp. 342-360.

Forsberg, R. and Sideris, M.G. (1993), Geoid computation by the multi-band spherical FFT approach, *Manuscript Geodesy*, Vol. 18, No. 2, pp. 82-90.

Forsberg, R. and Tscherning, C.C. (2008), *An Overview Manual for the GRAVSOFT Geodetic Gravity Field Modelling Programs*, DTU, Lyngby, Denmark.

Gilardoni, M., Reguzzoni, M., and Sampietro, D. (2016), GECO: a global gravity model by locally combining GOCE data and EGM2008, *Studia Geophysica Geodaetica*, Vol. 60, No. 2, pp. 228-247.

Heiskanen, W.A. and Moritz, H. (1967), *Physical Geodesy*, W.H. Freeman and Co., San Fransisco, C.A.

Hong, C.K., Kwon, J.H., Lee B.M., Lee, J., Choi Y.S., and Lee, S.B. (2009), Effects of gravity data quality and spacing on the accuracy of the geoid in South Korea, *Earth Planets Space*, Vol. 61, pp. 927-932.

ICGEM (2018), Root mean square (rms) about mean of GPS / levelling minus gravity field model derived geoid heights (m), *GFZ*, Potsdam, http://icgem.gfz-potsdam.de/tom_gpslev (last date accessed: 15 Jan 2018).

Iliffe, J.C., Ziebart, M., Cross, P.A., Forsberg, R., Strykowski G., and Tscherning C.C. (2003), OSGM02: a new model for converting GPS-derived heights to local height datums in Great Britain and Ireland, *Survey Review*, Vol. 37, No. 290, pp. 276-293.

Lee, S.B. and Kim, C.Y. (2011), Development of regional gravimetric geoid model and comparison with EGM2008 gravity-field model over Korea, *Scientific Research and Essays*, Vol. 7, No. 3, pp. 387-397.

Lee, J. and Kwon, J.H. (2015), Construction and precision verification of Korean national geoid model KNGeoid14, *Proceedings of the 2015 Spring Conference of the Korean Society of Surveying, Geodesy, Photogrammetry, and Cartography,* The Korean Society of Surveying, Geodesy, Photogrammetry, and Cartography, 23-24 April, Changwon, Korea, pp.177-179.

Lee, S.B. and Lee, D.H. (2010), Evaluation of the topographic effect using the various gravity reduction methods for precise geoid model in Korea, *International Association of Geodesy Symposia*, 23-27 June, Crete, Greece, Vol. 135, pp. 273-281.

Lee, S.B., Lee, K.S., and Lee, M.K. (2017), Analysis of the feasibility of GNSS/geoid technology in determining orthometric height in mountain, *Journal of the Korean Society for Geospatial Information Science*, Vol. 25, No. 2, pp. 57-65. (in Korean with English abstract)

Lee, D.H., Yun, H.S., Suh, Y.C., Hwang, J.S., and Min, B.I. (2012), KGEOID10: A new hybrid geoid model in Korea, *Proceedings of EGU General Assembly 2012, EGU, 22-27 April, Vienna, Austria, p. 7383.*

Omang, O.C.D. and Forsberg, R. (2000), How to handle topography in practical geoid determination: three examples, *Journal of Geodesy*, No. 74, pp. 458-446.

Pavlis, N.K., Holmes, S.A., Kenyon, S.C., and Factor, J.K. (2008), An earth gravitational model to degree 2160: EGM2008, *Proceedings of EGU General Assembly 2008, EGU, 13-18 April, Vienna, Austria, EGU2008-A-01891.*

Sjöberg, L.E. (2005), A discussion on the approximation made in the practical implementation of the remove-compute-restore technique in regional geoid modeling, *Journal of Geodesy*, No. 78, pp. 645-653.

SRTM (2000), Shuttle Radar Topography Mission, *NASA Jet Propulsion Laboratory*, California, http://www2.jpl.nasa.gov/srtm/ (last date accessed: 15 Aug 2012).